Synthesis, Bio-Evaluation, and HumanAbsorbed Dose Estimation of ^{68}Ga-Zoledronic Derivative for PET

Noshadi, Yashar
Radiation Application Department, Shahid Beheshti University, Tehran, I.R. IRAN

Sattarzadeh Khameneh, Elham
Radiation Application Research School, Nuclear Science and Technology Research Institute, Tehran, I.R. IRAN

Aghamiri, Seyyed Mahmoud Reza
Radiation Application Department, Shahid Beheshti University, Tehran, I.R. IRAN

Kakaei, Saeed*[*+]
Radiation Application Research School, Nuclear Science and Technology Research Institute, Tehran, I.R. IRAN

Yousefnia, Hasan
Radiation Application Research School, Nuclear Science and Technology Research Institute, Tehran, I.R. IRAN

Amraee, Naeimeh
Faculty of Engineering, Science and Research Branch, Islamic Azad University, Tehran, I.R. IRAN

ABSTRACT: *Today, the development of PET-based diagnostic radiopharmaceuticals is essential due to their accessibility by generators such as gallium-68 radioisotope. In this study, due to the distinctive properties of the bone-seeking agent of DOTA-ZOL, an effort is created to synthesize this valuable compound and use it in labeling with gallium-68. Further preclinical studies of ^{68}Ga-DOTA-ZOL are performed, and therefore the human absorbed dose after injection of the labeled compound was estimated based on rat biodistribution data. DOTA-ZOL was synthesized and characterized by FT-IR, NMR, and MS analyses. A tin-based in-house ^{68}Ge /^{68}Ga generator was used for labeling studies. To get the simplest labeling condition of DOTA-ZOL, completely different experiments were performed by variable labeling parameters together with concentration, time, pH, and time. The radiochemical purity of the radiolabeled complex was examined using RTLC methodology by totally different solvent systems. The steadiness of the final complex was assessed in PBS and human serum.*

*****To whom correspondence should be addressed.*
+ *E-mail: skakaei@aeoi.org.ir*
1021-9986/2023/8/2583-2593 *11/$/6.01*

The biodistribution of the radiolabeled complex as well as $^{68}GaCl_3$ was evaluated in normal rats up to 120 min post-injection. The human absorbed dose of the complex was estimated using animal data.^{68}Ga-DOTA-ZOL was prepared with radiochemical purity of quite 97 at optimized conditions using synthesized DOTA-ZOL and an in-house generator. The complex was stable in both PBS (4 ˚C) and in human blood serum (37 ˚C). The biodistribution studies in normal rats showed a high accumulation of ^{68}Ga-DOTA-ZOL injection with the most uptake at 30 min. The human absorbed dose estimation of the radiolabeled compound showed the highest absorbed dose was received by the bone tissue with the equivalent dose of 0.052 mGy/MBq. The results showed the attainable preparation of a new emerging bone-seeking agent of ^{68}Ga- DOTA-ZOL using an in-house generator. Also, the radiolabeled compound is considered an approximately safe radiopharmaceutical in terms of radiation absorbed dose.

KEYWORDS: *Gallium-68; Labeling compound; PET, Zoledronic derivative; Bone metastases; Dosimetry.*

INTRODUCTION

According to the World Health Organization's most current report data, malignant diseases get annually involve about four million people. Early cancers of the prostate, breast, lung, bladder, thyroid, lymphoma, and sarcoma are commonly associated with bone metastases. The metastases deeply affect the patient's quality of life and therefore, the treatment of bone abnormalities and the bone pain palliation of the patients have received much attention [1-5]. Chemists have been aware of bisphosphonates (BPs) since the mid-nineteenth century, with the first synthesis in 1865 in Germany [6]. Etidronate, the first BP used in humans to treat Paget's disease[7], was produced over a century ago [8]. In the early 1960s, William Neuman and Herbert Fleisch [9]investigated the causes of collagen induced calcification and discovered that body fluids such as plasma and urine contained inhibitors. Since it was discovered in the 1930s that polyphosphate might operate as water softeners by suppressing the crystallization of calcium salts such as calcium carbonate, they hypothesized that compounds of this type could be natural calcifies under physiological conditions. *Fleischet al.*[9, 10] discovered that inorganic pyrophosphate, a natural polyphosphate and a recognized byproduct of several metabolic activities in the body, is present in serum and urine and might inhibit calcification by adhering to freshly formed hydroxyapatite crystals. As a result, it was hypothesized that Proton Pump inhibitors (PPi) is the agent that ordinarily inhibits soft tissue calcification and controls bone mineralization. It was also hypothesized that various pathological disorders, such as kidney stones, may be associated with PPi metabolic disorders. Hydrolytic enzymes are thought to control the content of PPi in body fluids. These chemicals are made up of two groups of carbon-attached phosphonates which bind them to the bone's hydroxyapatite [11]. The general structure of these compounds is illustrated in Fig. 1.

The therapeutic effect of bisphosphonates and bone tendency in these substances is also due to two osteoporotic groups, R_1 and R_2 [12-15]. Bisphosphonates' analgesic properties and effectiveness for bone patients and their rate of excretion from the body are all affected by their structure, and even small alterations can have a substantial effect on these features [16, 17].

The US Food and Drug Administration has advised zoledronic acid to avoid skeletal events in patients with bone metastases, although several bisphosphonates have been evaluated in patients with solid tumors [18]. Zoledronic acid (Fig. 2) is a third-generation nitrogen bisphosphonate that can prevent bone problems in people with breast and prostate cancer [19]. When comparing laboratory findings between bisphosphonates, zoledronic acid had the highest bone resorption and the highest potential for osteoclasts binding [20, 21]. In fact, attractive features of zoledronic acid make it a promising option for new chemicals to detect bone metastases [22, 23].

^{99m}Tc-MDP and ^{99m}Tc-HMDP SPECT imaging agents have been widely employed as radiopharmaceuticals for the bone scan. Nowadays, due to the superiority of PET imaging over SPECT imaging, PET radiopharmaceuticals

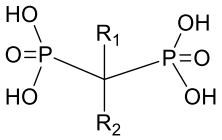

Fig.1: General structure of bisphosphonates

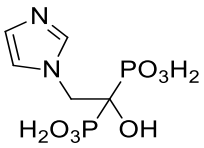

Fig.2: Chemical structure of zoledronic acid composition

are extensively improving. Gallium-68 with excellent physical properties [$T_{1/2}$ = 67.63 min; $E_{\beta+}$max = 1.92 MeV (89%); E_{γ} = 1077 keV (3.22%)] is currently recognized as one of the best radioisotopes for PET imaging in nuclear medicine [24]. On the other hand, ^{68}Ga is available in the form of ^{68}Ge /^{68}Ga generator and due to the long half-life of the parent's radioactive nucleus, it is inexpensive and easy to prepare and access in nuclear medical centers without the use of a cyclotron [25, 26].

Bisphosphonates, such as zoledronic acid, can be extensively used to prevent bone abnormalities and reduce the risk of fractures in malignancies such as prostate, breast, etc.[27]. The $^{68}Ga^{3+}$ cation can make high-specific-activity peptide tracers or other biomolecules connected to DOTA [26, 28]. Due to the special characteristics of zoledronic acid, as a bone seeking agent, and DOTA, as a chelator, DOTA-ZOL has been considered as an excellent carrier to transmit therapeutic dose to the bone metastases [29] and different therapeutic agents including ^{225}Ac-DOTA-ZOL, ^{177}Lu-DOTA-ZOL and ^{153}Sm-DOTA-ZOL have been developed for this purpose showed promising clinical results (Scheme 1) [30-32].

In this study, due to the excellent physical and chemical properties of ^{68}Ga PET radioisotope as well as its availability in the form of generator and the successful clinical results of DOTA-ZOL radiolabeled complexes, DOTA-ZOL bisphosphonate was first synthesized and evaluated. In order to study the efficiency of the synthesized DOTA-ZOL in performing diagnostic processes, the molecule was labeled with ^{68}Ga at optimized condition. After the quality control and stability studies of ^{68}Ga-zoledronic derivative, the biodistribution of bone seeking agent was evaluated in normal mice at different intervals. Finally, the human absorbed dose of the radiolabeled

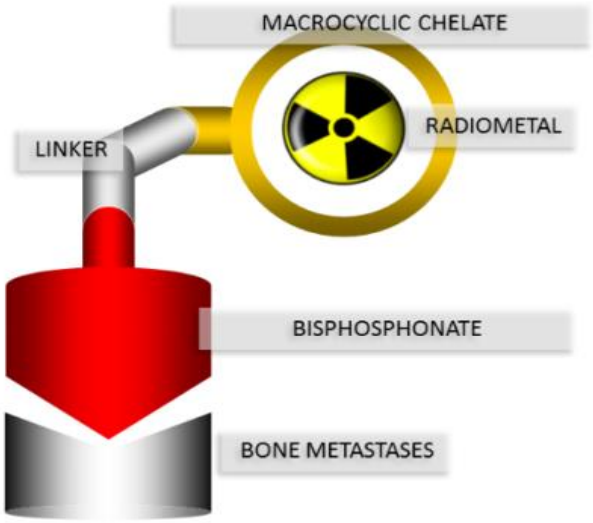

Sheme1: Schematic illustration of between phosphonates-based chelator like DOTA and chelator-conjugated BPs like Zoledronate

complex was estimated using Radiation Absorbed Dose Assessment Resource (RADAR) and *Spark et al*. methods.

EXPERIMENTAL SECTION

All reagents used in this study were purchased from Merck (Germany) and utilized without further purification. IR spectra were recorded on VECTOR 22 FT-IR spectrometer. Nuclear Magnetic Resonance (NMR) spectra was performed on Bruker DRX 300 MHz Spectrometer. The ^{68}Ge/^{68}Ga generator was obtained from Pars Isotope Co., Tehran, Iran. Dose calibrator device of model RAMS-88 (IRAN) was used for measuring the activity. For reading the paper chromatography and determination of radiochemical purity, Bioscan AR-2000 device (Bioscan Europe Ltd., France) and for determination of radionuclide purity, High Purity Germanium (p-type Coaxial EGPC 80-200-R) were used.

Synthesis of Zoledronic Acid derivative

Synthesis of 1-benzyl acetate-4-ethylamide imidazole

Nω-acetylhistamine 1g was initially dissolved in dry DMF (50) and cesium carbonate 4.4 g was added to the reaction mixture at 0°C. Benzylbromoacetate was added dropwise to the reaction, and the mixture stirred for another 12 h due to the formation of the yellow precipitate (Fig. 3). The product was purified and recrystallized with ethyl acetate.

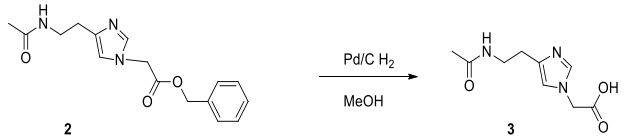

Fig.4: Synthesis of 1- acetic acid 4-ethyl acetamide imidazole

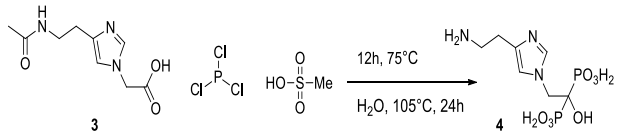

Fig.5: Synthesis of 4-ethylamino-1-hydroxyethyldidine bisphosphonic acid

Characterization of benzyl acetate-4-ethylamide imidazole

The reaction process was determined by TLC mixture of petroleum ether: ethyl acetate (PE: EA, 1:1) as the mobile phase, which produced a result of yellow crystals. Below are the spectra for this step of the synthesis.

Pale yellow crystals. Yield: 53%, m.p. 142-144 ^{o}C.^{1}H-NMR ($CDCl_3$, 300 MHz):δ 1.97 (s, 3H, CH_3-CO), 2.86 (t, J_H = 6.0 Hz, 2H, CH2-CH2), 3.55 (q, J_H = 6.0 Hz, 2H, CH_2-CH_2), 4.80 (s, 2H, N-CH_2-CO), 5.22 (s, 2H, Bn-CH_2-CO), 6.79 (bs, 1H, NH), 6.84 (d, J_H =1.3 Hz, imidazole-H), 7.38 (m, 5H, benzyl), 7.93 (d, J_H = 1.3 Hz, 1H, imidazole-H). IR (υ_{max}, cm^{-1}) 3245.4, 3052.7, 2936.7, 1715.5, 1370.9, 1199.1. ESIMS (+) m/z: calculated 301.34 found 302.15 $[M + H]^+$.

Synthesis of 1- acetic acid 4-ethyl acetamide imidazole (Hydrogenation reaction)

In this step, 1.5 g of synthesized compound in previous step (compound 2) was dissolved in 100 mL of dry methanol. Then 2.25 g palladium/carbon was added into the reaction mixture as a catalyst. The reaction mixture was exposed to a direct hydrogen gas flow for 24 h to reduction reaction occurred (Fig. 4). The acid (3) was used without further purification in the next step.

Characterization of 1-acetic acid 4-ethyl acetamide imidazole (resulting from hydrogenation)

The result of the second step of synthesis was identified using infrared and mass spectroscopy, as shown below.

Pale yellow crystals. Yield: 93%, m.p. 216-218 ^{o}C**.** IR (υ_{max}, cm^{-1}) 3475.4, 3252.7, 2936.7, 2936.7, 2418.4, 1625.5, 1390.9, 1159.1. ESIMS (+) m/z: calculated 211.22 found 210.48 $[M - H]^+$, 212.12 $[M + H]^+$.

Synthesis of 4-ethylamino-1-hydroxyethyldidine bisphosphonic acid

Previous step's product 208 mg and phosphorous acid164 mg were dissolved in methane sulfonic acid 1. Then phosphorus trichloride 300 mg was added dropwise to the mixture at 75˚C under argon atmosphere. The reaction continued for 36 hat room temperature. 2 of distilled water was added to the system. The reaction mixture is refluxed for 36 h with stirring. After the time has passed and the reaction stabilized using the TLC method, activated carbon added and mix for 5 min before filtering. A white precipitate develops with the addition of concentrated NaOH after the reaction temperature reached ambient temperature. After that, the mixture was stored in a fridge overnight to complete precipitation and filtered, washed with cold water and recrystallized from boiling water to obtain a white crystal product (Fig. 5).

Characterization of Ethylamino-1-hydroxyethyldidine bisphosphonic acid

IR and NMR spectroscopy were used to investigate and identify the result of this step. The spectra acquired in this stage are interpreted in the next section.

White crystals, Yield: 30%, m.p. 143-145 ^{o}C.^{1}H-NMR (D_2O/NaOD, 300 MHz): δ 2.48 (m, 2H, CH_2-CH_2), 2.69 (m, 2H, CH_2-CH_2), 3.42 (m, 2H, N-CH_2-phosponate), 6.99 (s, 1H, imidazole-H), 7.92 (s, 1H, imidazole-H). IR (υ_{max}, cm^{-1}) 3485.4, 3052.7, 2976.7, 1220.9, 1199.1. ^{31}P-NMR (D_2O/NaOD, 162.05 MHz): 14.4.

Synthesis of DOTA-ZOL

In this step, 50 mg of the preceding step's result was dissolved in hydrochloric acid (0.1 M, 0.6) at room temperature and 0.5 of triethylamine was added dropwise in to the mixture. Then, 50 mg of DOTA-NHS was dissolved in 0.4 of distilled water and added to the reaction. The reaction was agitated for 24 h in an oil bath at 35-40˚C. The unreacted zoledronic was removed by adding ethanol (Fig. 6). In the second step the crude product was purified further to remove DOTA impurities by Solid Phase Extraction (SPE). An aqueous solution of the compound was passed over a silica NH2-phase (Merck LiChroprep NH_2). After washing with water/methanol/water the product was eluted with H_2O + 2 % TFA.

DOTA-ZOL final product characterization

IR and NMR spectroscopy were also used to identify

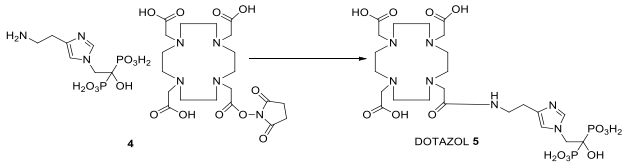

Fig.6: Synthesis of DOTA-ZOL

the final product.

Yellow crystals. Yield: 45%, m.p. 265-267 °C. IR (υ_{max}, cm^{-1}) 3483.4, 3252.5, 2876.7, 1627.6, 1424.4, 1129.3. ^{1}H-NMR (D_2O/NaOD, 300 MHz): 2.42 (m, 2H, CH_2-CH_2), 2.61 (m, 2H, CH_2-CH_2), 2.9.3.5 (b, 16H, cyclen-CH_2), 3.75 (bs, 8H, -CH_2-CO), 4.55 (m, 2H, N-CH_2-phosponate), 7.28 (s, 1H, imidazole-H), 8.54 (s, 1H, imidazole-H). ^{31}PNMR (D_2O/NaOD, 162.05 MHz): 14.3.

Mechanism of Synthesis

Based on the mechanism presented in Fig. ٧, the foremost necessary step of the reaction is expounded to the phosphorylation of the acid compound to a bisphosphonate via the reaction of a carboxylic acid with phosphorus trichloride in presents of methansolfonic acid (often called a condensation reaction), which we are going to justify during this step. The first step, is the reaction of the carboxylic acid (RCOOH) with phosphorous trichloride, forming the acid chloride. The reaction continues with a nucleophilic attack to the carbonyl group of acid chloride by an anhydride intermediate Cl_2P-O-SO_2Me (formed by the reaction between MSA and phosphorous trichloride Scheme). As a result, upon the loss and Cl^-, it is transformed into the corresponding keto intermediates. These stable forms can then react with another molecule of Cl_2P-O-SO_2Me, leading to the formation of the last intermediate. In the final steps, its hydrolysis allows to obtain the targeted BP.

Preparation and quality control of gallium-68

An in-house tin oxide-based $^{68}Ge/^{68}Ga$ generator was employed for this study. The generator was eluted by 0.1 M HCl acid (2) and ^{68}Ga radioisotope was prepared in the form of $^{68}GaCl_3$. Chemical, radiochemical and radionuclide purities of the elution were investigated using ICP-Mass, Bioscan and HPGe devices, respectively. The radiochemical purity of $^{68}GaCl_3$ was investigated using thin layer chromatography in two different solvent systems of DTPA (10 mM) and 10% ammonium acetate:methanol (1:1) as the mobile phases and Whatman paper No. 1 as the stationary

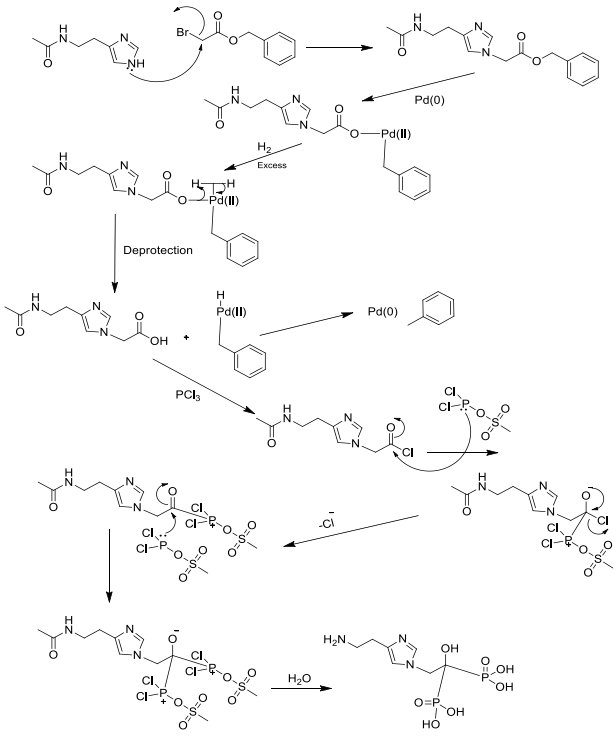

Fig.7: Mechanism of reaction

phase. The radionuclide purity of the radioisotope was assessed both after elution and after 24 h post elution to detect any possible eluted germanium-68 [33, 34].

Preparation and quality control of ^{68}Ga-DOTA-ZOL

Various experiments were performed by varying labeling parameters to label DOTA-ZOL with gallium-68 at optimized conditions. Temperature, acidity, reaction time, and material concentration were explored as possible factors impacting the labeling process. The DOTA-ZOL complex was dissolved in 1 M sodium acetate buffer to prepare a stock solution (1 mg/). To investigate the effect of the mentioned parameters; at the first step, identical quantities of DOTA-ZOL complex and gallium-68 activity were put into 10 vials. The pH of the reactions was adjusted from 2 to 6 and the radiochemical purity of the reactions was assessed at different intervals. At the second step, different values of the complex were considered with the same activities for the appropriate ph. The radiochemical purity of the labeled compound was evaluated using different solvent systems: 1) Acetyl acetone: acetone: HCl (37%) (10:10:1); 2) NH_4OH, methanol, and water in ratios (0.2, 2, and 4); 3) Sodium citrate 0.25 M, pH = 4; 4) Ammonium acetate, methanol in ratio (50: 50).

Stability of the complex

The stability of the radiolabeled complex was assessed in PBS buffer (4˚C) for up to 2 h. For this purpose, a of the sample ^{68}Ga-DOTA-ZOL labeled compound was maintained and the radiochemical purity of the sample was assessed using the RTLC technique at 15, 30, 60, and 120 min. In addition, to study the serum stability of the final compound, fresh serum (500 µL) was added to a sample of the labeled compound and stored at 37˚C for up to 2 h. The radiochemical purity of the sample was assessed using the RTLC technique at 15, 30, 60, and 120 min.

Bio-distribution studies of $^{68}GaCl_3$ and ^{68}Ga-DOTA-ZOL in normal rats

The biological distribution of $^{68}GaCl_3$ and ^{68}Ga-DOTA-ZOL was studied in rats weighting 140-160 g and aged 8-10 weeks. $^{68}GaCl_3$ solution (200 µl) and the ^{68}Ga-DOTA-ZOL (200 µl) with approximately 7.4MBq activity were administered intravenously into the tail vein of the normal rats (n=4). Syringe activity was measured before and after injection to calculate total injection activity in each animal. The animals were sacrificed at 15, 30, 60, and 120 min after injection and the blood samples were quickly collected. The tissues including heart, kidneys, spleen, stomach, intestine, lung, liver, skin, bone, muscle, thyroid, adrenal glands, salivary glands, and pancreas were weighed and rinsed with the water. The activity of each tissue was measured by a p-type coaxial HPGe detector coupled with a multi-channel analyzer based on Equation 1.

$$A = \frac{N}{\epsilon \gamma t_s\, m k_1 k_2 k_3 k_4 k_5} \quad (1)$$

Where ϵ is the efficiency at photopeak energy, γ *i*s the emission probability of the gamma line corresponding to the peak energy, t_s is the sample spectrum collection live time in seconds, *m* is the mass (kg) of the measured sample, and k_1, k_2, k_3, k_4, k_5 are the correction factors for the nuclide decay since the time of sample collection for starting the measurements, the nuclide decay during the counting period, self-attenuation in the measured sample, *N* denotes the adjusted net peak area of the relevant photopeak, which is computed as follows:

$$N = N_s \frac{t_s}{t_b} N_b \quad (2)$$

N_s is the sample spectrum's net peak area, N_b is the background spectrum's corresponding net peak area, and t_b is the background spectrum collection's live time in seconds. The ID/gr% for each organ is computed using following equations:

$$\frac{\text{ID}}{\text{gr}}\% = \frac{\text{Activity (Bq)}}{A(t)\ \text{(Bq)} \times \text{Tissue weight (gr)}} \times 100 \quad (3)$$

In the above relation, *A (t)* is the total injection activity, and tissue weight is the weight of each tissue. In addition, the activity of each tissue is deducted from the following equation. The area is the number read by the detector, *t* is the counting time in seconds, eff is the detector efficiency, and Br is the abundance of the gamma-ray counted.

$$activity = \frac{area}{t \times eff \times Br \times 37000} \quad (4)$$

Statistical analysis

The uncertainty in activity measurement was calculated using the error propagation formula, which is given below:

$$\sigma_x^2 = \frac{\sum_{i=1}^{N} \sigma_{x_i}^2}{N} \quad (5)$$

Where σ_{xi} is the degree of uncertainty in each experiment and N denotes the number of experiments for each organ, the percentage of the injected dose per gram (percent ID/g) was computed by dividing the quantity of activity in each tissue (A) by the decay-corrected injected activity and the mass of each organ. At each time period, four rats were sacrificed. The data were compared using the student's t-test after all values were represented as mean standard deviation.

Calculation of absorption dose in humans based on animal data

The most generally utilized approach of determining the human dosage from animal data is an extrapolation from the relative mass of the organ. RADAR method is the mostly used method for internal dose assessment of the radiopharmaceuticals. The absorbed dose in the target organ T from the radionuclide in a single source organ *S* is obtained from Equation (6).

$$D(T \leftarrow S) = \check{A}_s \times S(T \leftarrow S) \quad (6)$$

Equation (7) was used to calculate the accumulated source activity for each animal source organ, where *A (t)* is the activity of each organ at time t;

$$\tilde{A}_s(t) = \int_0^t A_s\,(u)\,du \quad (7)$$

Data points representing the non-decay corrected percentage of the injected dose were created for this purpose. Between the two experimental time points, a linear

Table 1: Investigation of the effect of catalyst content on hydrogenation reaction efficiency

Test	Catalyst rate(%w)	Time(h)	Product efficiency%
1	0	24	25
2	2	24	30
3	5	24	45
4	8	24	52
5	10	24	80
6	15	24	93
7	20	24	92
8	30	24	90
9	35	24	89

Table 2: Investigation of the effect of temperature changes on the efficiency of hydrogenation reaction

Temperature ºC	25	35	45	60	70	80
Yield %	93	90	88	76	40	33

approximation was used. By fitting the tail of each curve to a mono-exponential curve with an exponential coefficient equal to the physical decay constant of ^{68}Ga, the curves were extrapolated to infinity. Using a method proposed by *Sparks et al*. (Equation8) and the standard mean weight of each human organ, the accumulated activity in animals was calculated [35, 36].

$$\tilde{A}_{human\ organ} = \tilde{A}_{animmal\ organ} \frac{Organ\ Mass_{human}/Body\ Mass\ human}{Mass Organ\ Mass_{animal}/Body\ Mass_{animal}} \quad (8)$$

RESULTS AND DISCUSSION

Optimization of hydrogenation reaction conditions

The catalyst values were investigated in order to reach ideal circumstances. The best results were achieved when 15%W of palladium/carbon catalyst was used at 25˚C (Table 1). Due to the generation of by-products, the reaction efficiency dropped as the catalyst rose.

The reaction was carried out at various temperatures, ranging from ambient temperature to 80˚C, to evaluate the influence of temperature on hydrogenation efficiency, as indicated in Table 2. The outcome of the reaction was assessed using thin-layer chromatography. It shows that the reaction efficiency at room temperature is 93 % and that as the temperature rises, the labeling reaction efficiency drops from 90% to 33%. As a consequence, increasing the temperature does not only raise but also reduce the efficiency, and as a result, the temperature does not influence on reaction efficiency.

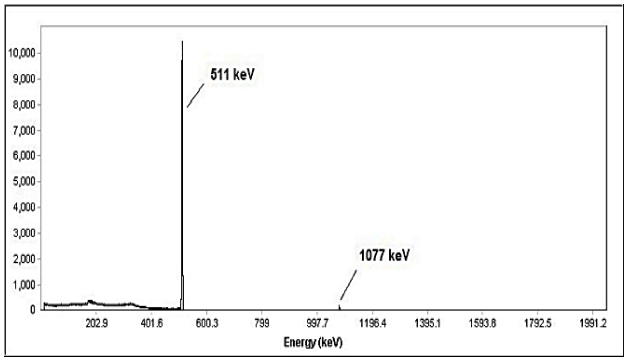

Fig.8: Gamma spectrum obtained from gallium chloride-68 by HPGe detector

Preparation and quality control of gallium chloride-68

0.1MHCl acid was used for effective washing of the generator. The first 0.5 of the cleaning products was thrown away, and the remaining 2 was utilized to label the bottles. Tin, zinc, and copper concentrations in ^{68}Ga eluted from the generator were determined by ICP-OES< 0.1 ppm. The gamma spectroscopy revealed the existence of two gamma rays with an energy of 511 and 1077 keV all originating from ^{68}Ga (Fig. 8). The eluted ^{68}Ge from the generator was also less than 0.001% which is in acceptable level. The radiochemical purity of the $^{68}GaCl_3$ sample assessed using two different solvent systems was more than 99% (Fig. 9) [34].

Preparation and quality control of labeled compound

Under several circumstances, the labeling procedure was performed to obtain the optimal DOTA-ZOL labeling efficiency with Gallium-68. ^{68}Ga-DOTA-ZOL was prepared with radiochemical purity of more than 97 % at optimized condition. The best labeling conditions was as follows: 25 µg of DOTA-ZOL ligand was dissolved in 500 µL of 1M sodium acetate buffer (pH = 4.5) and mixed with 1.5 of $^{68}GaCL_3$. The reaction solution was stirred for 30 min at 98°C and the final pH was adjusted to 4.

RTLC chromatography was used to determine the radiochemical purity of radiolabeled compound. Acetyl acetone:acetone:HCl (37%) (10:10:1) were considered as the appropriate mobile phase. In this system, the free gallium stays at the origin and the labeled compound migrates to the higher R_fs (Fig. 10).

Stability tests in PBS buffer and in human serum

The radiochemical purity of ^{68}Ga-DOTA-ZOL in PBS buffer (4 °C) and in human blood serum was assessed

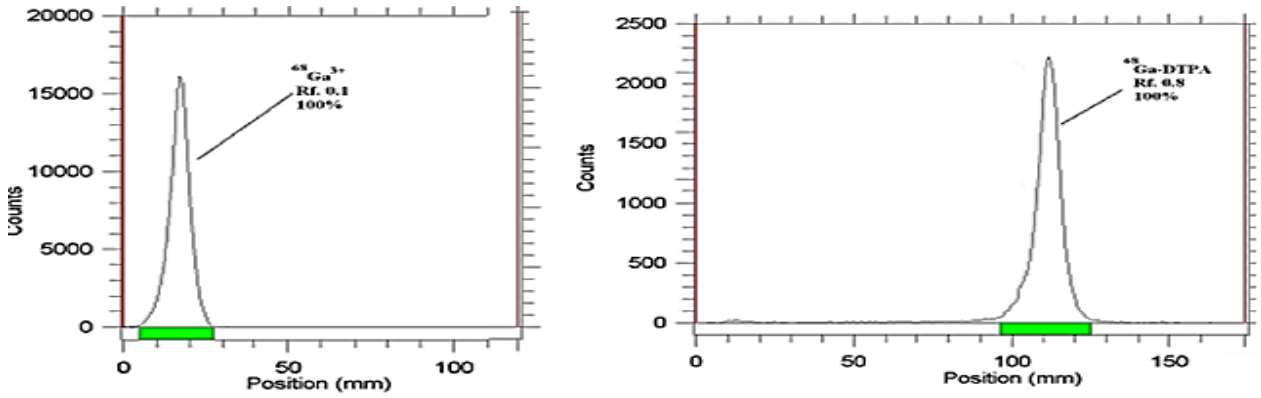

Fig.9: ITLC chromatogram of $^{68}GaCl_3$ in DTPA with 10 mM concentration and acidity 5 (right) and ammonium acetate 10%: methanol (1: 1) (left) in Watman No. 2

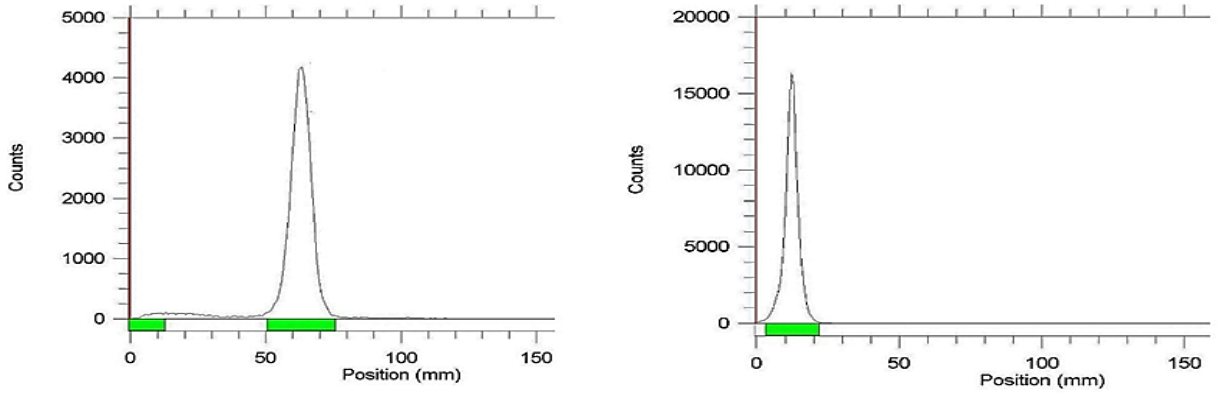

Fig.10: RTLC chromatograms of free gallium (left) and ^{68}Ga-DOTA-ZOL (right) in acetyl acetone:acetone:HCl (37%) (10:10:1) solvent system

least for 2 h. The radiochemical purity of the radiolabeled compound was determined to be greater than 98 % even 2 h post preparation.

Biodistribution of $^{68}GaCl_3$and ^{68}Ga-DOTA-ZOL in normal rats

The biological distribution of $^{68}GaCl_3$ in normal rats has been investigated for control studies of the bio distribution of labeled compounds. The percentage of injection dose per gram of the tissues was determined up to 120 min post injection (Fig. 11). The biodistribution of the ^{68}Ga-DOTA-ZOL radiolabeled complex was also studied for 120 min (Fig. 12).

As it can be seen, the major remained activity of the radiolabeled compound accumulated in the bone tissue and the maximum activity accumulation occurs in 30 min post injection. Also, the uptake of the kidneys and the bladder shows that the urinary track is the main route of excretion of the bone seeking agent.

Human absorbed dose estimation of the ^{68}Ga-DOTA-ZOL

The RADAR formulas were used to estimate the equivalent and effective dose of various human organs after injection of^{68}Ga-DOTA-ZOL radiopharmaceutical (Table 3). As expected, the highest absorbed dose is received by the bone tissue with the equivalent and effective dose of0.052 mGy/MBq and 0.001mSv/MBq, respectively. The effective dose of total body was 0.005 mSv/MBq.

CONCLUSIONS

In this piece of research work, DOTA-ZOL was successfully synthesized and was evaluated using IR, NMR, Mass Spectrometry, etc. The bone seeking agent was labeled with ^{68}Ga prepared from an in-house ^{68}Ge/^{68}Ga generator with radiochemical purity of greater than 97% at optimized condition. The final radiolabeled compound was stable in both PBS (4°C) and in human blood serum (37°C). The biodistribution studies in normal rats showed high

Table 3: Equivalent and effective absorbed dose delivered into human organs after injection of 68Ga-DOTA-ZOL

Target Organs	Equivalent absorbed dose (mGy/MBq)	W_{ta}	Effective absorbed dose (mSv/MBq)
Adrenals	0.0 02	0.12	0.000
Brain	0.002	0.01	0.000
GB Wall	0.001	0.12	0.000
LLI Wall	0.001	0.12	0.000
Small Int	0.002	0.12	0.000
Stomach Wall	0.001	0.12	0.000
ULI Wall	0.001	0.12	0.000
Heart Wall	0.001	0.12	0.000
Kidneys	0.008	0.12	0.001
Liver	0.002	0.04	0.000
Lungs	0.002	0.12	0.000
Muscle	0.001	0.12	0.000
Pancreas	0.001	0.12	0.000
Red Marrow	0.046	0.12	0.006
Bone Surf	0.052	0.01	0.001
Spleen	0.010	0.12	0.001
Testes	0.001	0.12	0.000
Thymus	0.001	0.12	0.000
Thyroid	0.001	0.04	0.000
UB Wall	0.026	0.04	0.001
Total Body	0.005		0.005

GW: Gallbladder Wall; LLI: lower large intestine; Int: Intestine; ULI: upper large intestine; UB Wall: Urinary Bladder Wall.

[a]Tissue weighting factors according to international commission on radiological protection, ICRP 103 (2007).

accumulation of the radiolabeled compound in the bone tissue even after 15 min post injection with the maximum uptake at 30 min. The human absorbed dose estimation of ^{68}Ga- DOTA-ZOL demonstrated the highest absorbed dose is received by the bone tissue with the equivalent dose of 0.052 mGy/MBq. As the effective dose of total body was estimated to be 0.005 mSv/MBq, this radiolabeled compound can be considered as an approximately safe radiopharmaceutical in terms of radiation dose.

Acknowledgments

The authors gratefully acknowledge the support of the present work by Radiation Application Research School, Nuclear Science & Technology Research Institute, P.O. Box 11365-3486.

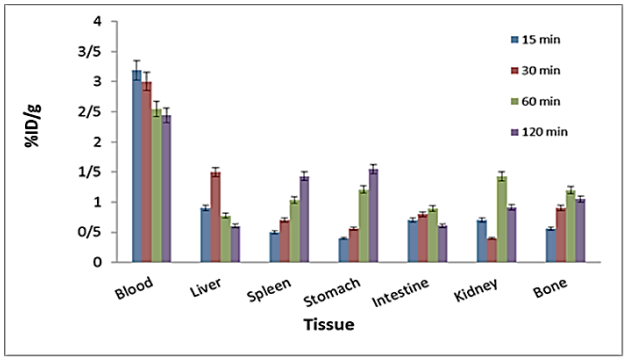

Fig.11: Percentage of injection dose per gram of $^{68}GaCl_3$ in normal rats at different intervals

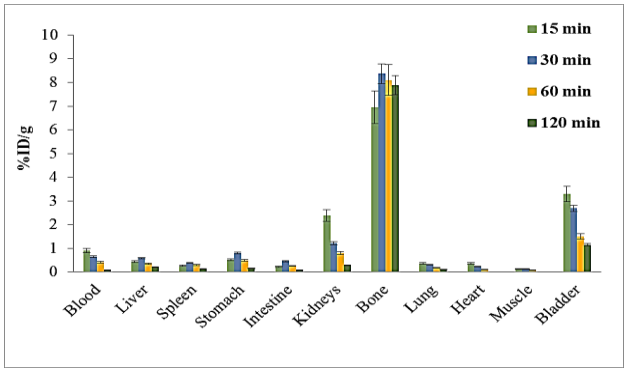

Fig.12: Percentage of injection dose per gram in healthy rats in terms of time after ^{68}Ga-DOTA-ZOL injection

List of the abbreviation

PET	Positron Emission Tomography
SPECT	Single-Photon Emission Computerized Tomography
DOTA	2, 2′, 2″, 2‴-(1, 4, 7, 10-Tetraazacyclododecane-1, 4, 7, 10-tetrayl) tetra acetic acid
FT-IR	Fourier Transform Infrared Spectrometer
NMR	Nuclear Magnetic Resonance
MS	Mass Spectroscopy
RTLC	Radio Thin Layer Chromatographic
PBS	Phosphate-Buffered Saline
BPs	Bisphosphonates
PPi	Proton Pump inhibitors
MDP	Methylene Diphosphonate
HMDP	HydroxymethyleneDiphosphonate
RADAR	Radiation Absorbed Dose Assessment Resource
DMF	Dimethylformamide
PE	Petroleum Ether
EA	Ethyl Acetate
SPE	Solid Phase Extraction

MSA	Methanesulfonic acid
ICP	Inductively Coupled Plasma
DTPA	Diethylenetriamine penta acetic acid

Received : Sep. 24, 2022 ; Accepted : Dec. 19, 2022

REFERENCES

[1] Kuźnik A., Październiok-Holewa A., Jewula P., Kuźnik N., Bisphosphonates—Much More than Only Drugs for Bone Disease, *European Journal of Pharmacology*, **866**: 172773 (2020).

[2] Yang M., Yu X., Management of Bone Metastasis with Intravenous Bisphosphonates in Breast Cancer: A Systematic Review and Meta-Analysis of Dosing Frequency, *Supportive Care in Cancer*, **28**: 2533-2540 (2020).

[3] Abdussalam-Mohammed W., Review of Therapeutic Applications of Nanotechnology in Medicine Field and its Side Effects, *Journal of Chemical Reviews*, **1**: 243-251 (2019).

[4] Hosseinzadeh Z., Ramazani A., Razzaghi-Asl N, Plants of the Genus Heracleum as a Source of Coumarin and Furanocoumarin, *Journal of Chemical Reviews*, **1**: 78-98 (2019).

[5] Peddagundam B., Abdul Ahad H., Chinthaginjala H., Ksheerasagare T., Ganthala A K., Gummadisani G.R., The Design of Soft Drugs: Basic Principles, Energetic Metabolite Methods, Approved Compounds, and Pharmaceutical Applications, *Journal of Chemical Reviews*, **4**: p. 241-254 (2022).

[6] Menschutkin N., Ueber Die Einwirkung Des Chloracetyls Auf Phosphorige Säure, *Justus Liebigs Annalen der Chemie*, **133**: 317-320 (1865).

[7] Smith R., Russell R., Bishop M., Diphosphonates and Paget's Disease of Bone, *The Lancet*, 297, p. 945-947 (1971).

[8] Von Baeyer H., Hofmann K., Acetodiphosphorige Saure, *Beitr Dtsch Chem Ges*, **30**: 1973-1978 (1897).

[9] Fleish H., Neuman W.F., Mechanisms of Calcification: Role of Collagen, Polyphosphates, and Phosphatase, *American Journal of Physiology-Legacy Content*, **200**: 1296-1300 (1961).

[10] Fleisch H., Russell R., A Review of the Physiological and Pharmacological Effects of Pyrophosphate and Diphosphonates on Bones and Teeth, *Journal of Dental Research*, **51**: 323-332 (1972).

[11] Russell R., Hodgkinson A., The Urinary Excretion of Inorganic Pyrophosphate by Normal Subjects and Patients with Renal Calculus, *Clinical Science*, **31**: 51-62 (1966).

[12] Farrell K B., Karpeisky A., Thamm D H., Zinnen S., Bisphosphonate Conjugation for Bone Specific Drug Targeting, *Bone Reports*, **9**: 47-60 (2018).

[13] Maghsoudi S., Hosseini S.A., Ravandi S., A Review on Phospholipid and Liposome Carriers: Synthetic Methods and Their Applications in Drug Delivery, *Journal of Chemical Reviews*, **4**: 346-363 (2022).

[14] Kakanejadifard A., Synthesis, Characterization, Crystal Structure and Density Functional Investigation of Dialkyl(Phenyl((4-(Phenyl Diazenyl)Phenyl) Amino)Methyl) Phosphonate, ***333174****:* (2021).

[15] Faghihian H.,Yaghobb Nejadasl H., Synthesis, Characterization and Application of a Novel Zirconium Phosphonate Ion-Exchanger for Removal of Ni^{2+}, Cu^{2+} and Zn^{2+} from Aqueous Solutions, *333174*. **30**: 23-31 (2011).

[16] Russell R.G.G., Bisphosphonates: From Bench to bedside, *Annals of the New York Academy of Sciences*, **1068**: 367-401 (2006).

[17] J Roelofs A., Thompson K., H .Ebetino F., J. Rogers M., P Coxon F., Bisphosphonates: Molecular Mechanisms of Action and Effects on Bone Cells, Monocytes and Macrophages, *Current Pharmaceutical Design*, **16**: 2950-2960 (2010).

[18] Edwards B.J., Gounder M., McKoy J.M., Boyd I., Farrugia M., Migliorati C., Marx R., Ruggiero S., Dimopoulos M., Raisch D.W, Pharmacovigilance and Reporting Oversight in US FDA Fast-Track Process: Bisphosphonates and Osteonecrosis of the Jaw, *The Lancet Oncology*, **9**: 1166-1172 (2008).

[19] Heymann D., Ory B., Gouin F., Green J.R., Rédini F., Bisphosphonates: New Therapeutic Agents for the Treatment of Bone Tumors, *Trends in Molecular Medicine*, **10**: 337-343 (2004).

[20] Ponte Fernández N., Estefania Fresco R., Aguirre Urizar J.M., Bisphosphonates and Oral Pathology I. General and Preventive Aspects, *Medicina Oral, Patologia Oral Y Cirugia Bucal*, **11**: E396-400 (2006).

[21] Mbese Z., Aderibigbe B.A., Bisphosphonate-Based Conjugates and Derivatives as Potential Therapeutic Agents in Osteoporosis, Bone Cancer and Metastatic Bone Cancer, *International Journal of Molecular Sciences*, **22**: 6869 (2021).

[22] Isla D., Afonso R., Bosch-Barrera J., Martínez N., Zoledronic Acid in Lung Cancer with Bone Metastases: A Review, *Expert Review of Anticancer Therapy*, **13**: 421-426 (2013).

[23] Coleman R., Cook R., Hirsh V., Major P., Lipton A., Zoledronic Acid Use in Cancer Patients: More than Just Supportive Care? *Cancer*, **117**: 11-23 (2011).

[24] Wadsak W., Mitterhauser M., Basics and Principles of Radiopharmaceuticals for PET/CT, *European Journal of Radiology*, **73**: -469 (2010).

[25] Sudbrock F., Fischer T., Zimmermanns B., Guliyev M., Dietlein M., Drzezga A., Schomäcker K., Characterization of SnO_2-Based $^{68}Ge/^{68}Ga$ Generators and ^{68}Ga-DOTATATE Preparations: Radionuclide Purity, Radiochemical Yield and Long-Term Constancy, *EJNMMI Research*, **4**: 1-10 (2014).

[26] Velikyan I., Prospective of 68Ga-Radiopharmaceutical Development, *Theranostics*, **4**: 47 (2014).

[27] Ogawa K., Saji H., Advances in Drug Design of Radiometal-Based Imaging Agents for Bone Disorders, *International Journal of Molecular Imaging*, **2011** (2011).

[28] Bandoli G., Dolmella A., Tisato F., Porchia M., Refosco F., Mononuclear Six-Coordinated Ga (III) Complexes: A Comprehensive Survey, *Coordination Chemistry Reviews*, **253**: 56-77 (2009).

[29] Farhanghi M., Holmes R.A., Volkert W.A., Logan K.W., Singh A., Samarium-153-EDTMP: Pharmacokinetic, Toxicity and Pain response Using an Escalating Dose Schedule in Treatment of Metastatic Bone Cancer, *J. Nucl. Med.*, **33**: 1451-1458 (1992).

[30] Pfannkuchen N., Bausbacher N., Pektor S., Miederer M., Rosch F., In Vivo Evaluation of [^{225}Ac] Ac-Dotazol for α-Therapy of Bone Metastases, *Current Radiopharmaceuticals*, **11**: 223-230 (2018).

[31] Yadav M.P., Ballal S., Meckel M., Roesch F., Bal C., [^{177}Lu] Lu-DOTA-ZOL Bone Pain Palliation in Patients with Skeletal Metastases from Various Cancers: Efficacy and Safety Results, *EJNMMI Research*, **10**: 1-13 (2020).

[32] Yen N., Azahari K., Wan H.B.W.K., Choong K.K., Radiolabelling and Preliminary Biodistribution Study of Samarium-153-Zoledronic Acid as a Novel Bone Pain Palliative Agent.

[33] Sattarzadeh E., Amini M.M., Kakaei S., Khanchi A., ^{68}Ga-radiolabeled Magnetic Nanoparticles for PET–MRI Imaging, *Journal of Radioanalytical and Nuclear Chemistry*, **317**: 1333-1339 (2018).

[34] Tayeri H.R., Sattarzadeh Khameneh E., Zolghadri S., Kakaei S., Sardari D., Optimized Production, Quality Control and Biological Assessment of 68-Ga-Bleomycin as a Possible PET Imaging Agent, *International Journal of Radiation Research*, **18**: 235-241 (2020).

[35] Sparks R., Aydogan B, "Comparison of the Effectiveness of some Common Animal Data Scaling Techniques in Estimating Human Radiation Dose", Oak Ridge Associated Universities, TN (United States) (1999).

[36] Stabin M G.,Siegel J A, Physical Models and Dose Factors for Use in Internal Dose Assessment, *Health Physics*, **85**: 294-310 (2003).